Reproduction of Thermal Plume above Commercial Cooking Gas Stove using CFD Analysis

Takao OSAWA [a], *Takashi KURABUCHI* [b], *Yoshihiro TORIUMI* [c], *Sihwan LEE* [d], *Yuki SHIMANUKI* [e] , *Ami KUDO* [f]

[a] Graduate Student, Department of Architecture, Faculty of Engineering, Tokyo University of Science, Japan, takao1089@gmail.com

[b] Professor, Department of Architecture, Faculty of Engineering, Tokyo University of Science, Japan, kura@rs.tus.ac.jp

[c] Professor, Division of Architectural, Civil and Environmental Engineering School of Science and Engineering, Tokyo Denki University, Japan, toriumi@g.dendai.ac.jp

[d] Associate Professor, Graduate School of Environmental Studies, Nagoya University, Japan, shany@nuac.nagoya-u.ac.jp

[e] Researcher, TOKYO GAS CO.,Ltd, Japan, n-yuki@tokyo-gas.co.jp

[f] M.Technol. Manag. , TOKYO GAS CO.,Ltd, Japan, Kudo_ami@tokyo-gas.co.jp

Abstract. In commercial kitchens, the working environment of cooks deteriorates because of the generation of large amounts of heat and vapor. Ventilation is required to improve the environment, and the accompanying increase in air-conditioning energy becomes an issue. Therefore, a proper ventilation design is required to reduce the risk of contaminated air, thereby deteriorating the indoor environment. When planning ventilation and air conditioning for commercial kitchens, the heat generated by cooking products can be efficiently exhausted to reduce the air conditioning load and maintain good air quality in the workspace. Computational fluid dynamics (CFD) analysis was used to predict the air conditioning load and air quality. It is important to accurately evaluate the heat generated from the cooking equipment and the exhaust collection performance of cooking products. At that time, the accuracy of reproducing the thermal updraft is important, but when the capture efficiency is predicted using the simple gradient diffusion hypothesis model, which is widely used for indoor airflow analysis, the capture efficiency is excess owing to insufficient diffusion. Several studies on the thermal plume on gas stoves have been conducted thus far[1]–[4], and previous studies have clarified that there is a problem in the reproducibility of the production term G_k owing to the buoyancy of the turbulent kinetic energy. It is possible to improve the accuracy using the generalized gradient diffusion hypothesis (GGDH), which uses the gradient of the average flow other than the diffusion direction as the approximation method for the turbulent heat flux in G_k. In this study, we investigated the reproducibility of CFD analysis with a GGDH on an open fire. First, we measured the thermal plume and capture efficiency. Subsequently, as a result of attempting to reproduce the thermal plume with CFD and then perform capture efficiency analysis, it was confirmed that the actual measurement results were consistent with the analysis results. Because the actual measurement and CFD results were in agreement, we believe that it would contribute to comfort and energy savings in a commercial kitchen.

Keywords. Capture efficiency, Commercial kitchen, Thermal plume, CFD
DOI: https://doi.org/10.34641/clima.2022.324

1. Introduction

An appropriate ventilation design is required to maintain the optimum working environment in a commercial kitchen, and the recovery efficiency of the hood exhaust is an important index.

The capture efficiency of the hood exhaust indicates the amount of pollutant generated by kitchen equipment that can be collected by the exhaust hood.

The purpose of this research is to examine the reproducibility of computational fluid dynamics (CFD) from the temperature measurement and capture efficiency measurement of the heat updraft in the direct flame and to propose a CFD analysis when the pot is placed in the future.

2. Reproduction of thermal plume

2.1 Measurement overview

The temperature and velocity distributions were obtained by measuring the temperature of the thermal plume. **Figure 1** shows a plan view of the environmental test room used for the measurement.

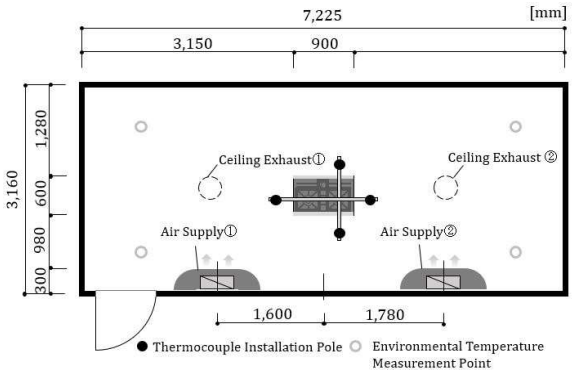

Fig. 1 – Environmental test room (floor plan)

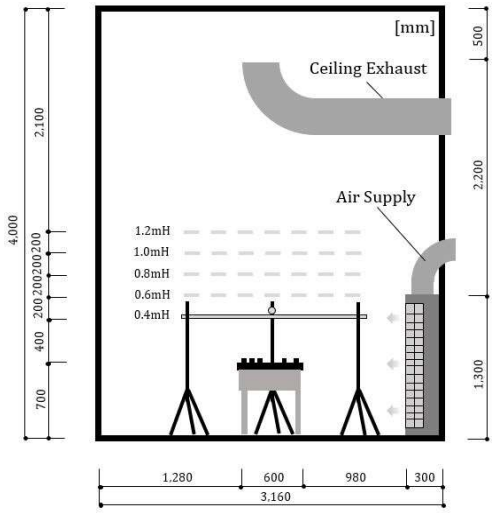

Fig. 2 – Environmental test room (cut open)

A commercial gas stove is installed at the center of the room, and one of the three is used for measurement. **Figure 2** shows a cross-sectional view. The measurement heights were 0.4, 0.6, 0.8, 1.0, and 1.2 m from the burner. **Figure 3** shows the locations of the measurement points.

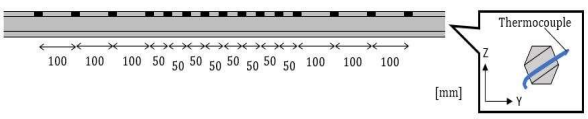

Fig. 3 – Installation position of thermocouple

Based on the lower heating value of 12.7 kW corresponding to the rated output, the thermal power was set to three conditions of 9.2 and 4.6 kW, which correspond to two-thirds and one-third of the rated output, respectively. For velocity distribution, the central velocity v_c was calculated using **Eq. (1)**, where the low calorific value of the city gas is taken as the retained calorific value H of the plume, ρ denotes the density, c_p is the specific heat, t_c is the temperature difference on the central axis, and v_c is the velocity on the central axis. The distribution widths R_t and R_v denote the radial distances of the points where the central axis temperature and central axis velocity are 1/e, and the ratio of R_t and R_v expressed in **Eq. (2)** is 0.9.

$$H = \pi\rho c_p t_c v_c \frac{R_t^2 R_v^2}{R_t^2 + R_v^2} \quad \cdots(1)$$

$$\lambda = R_t / R_v \quad \cdots(2)$$

The measurements were performed under the condition of an open fire without a pot.

2.2 Boundary conditions for CFD analysis

Figure 4 shows an outline of the analysis model, and **Tab. 1** lists the boundary conditions for plume analysis.

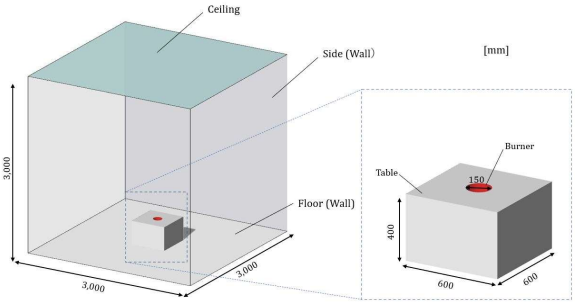

Fig. 4 – CFD analysis model of thermal plume

Tab. 1 – Boundary conditions (plume analysis)

Boundary	Type		
burner	4.6 kW	Temperature	516 ℃
		Velocity	1.16 m/s
	9.2 kW	Temperature	810 ℃
		Velocity	2.00 m/s
	12.7 kW	Temperature	1002 ℃
		Velocity	2.62 m/s
	Material: Air Turbulent intensity: 0.25 Turbulent length scale: 0.10 m		
Floor	All dependent variable : 0 gradient condition		
Ceiling	Boundary (Pressure: 0.00 Pa)		
Side	All dependent variable : 0 gradient condition		
Table	All dependent variable : 0 gradient condition		

The boundary conditions for plume analysis were set based on the actual experimental results. The burner diameter was set to 0.15 m. The temperature of the burner was 516 °C when the calorific value was 4.6 kW. In addition, based on the similarity rule of Maele et al.[5], we set the stove temperature to 1002 °C at 12.7 kW, and calculated the velocity at each thermal power by back calculation from **Eq. (3)**.

$$H = c_p \rho A v \Delta\theta \quad \cdots(3)$$

Table 2 lists the analysis conditions. The total number of meshes was 980,000 meshes.

Tab. 2 – Analysis conditions

	Analysis conditions
Software	Simcenter STAR-CCM+ 2020.3
Turbulence	Standard k-ε Model Generalized k-ε Model
Density	Incompressible ideal gas
Algorithm	Time dependent
Mesh	980,000 meshes
Analysis area	3,000mm(X)×3,000mm(Y)× 3,000mm(Z)

2.3 Turbulence model

The turbulence model used in this study is explained. Simple gradient diffusion hypothesis (SGDH) and generalized gradient diffusion hypothesis (GGDH) were used as the turbulence models, and the reproducibility of the thermal plume was compared with the measured results. **Table 3** lists the turbulence model formula. **Equation (4)** is the transport equation for the turbulent kinetic energy k, and **Eq. (5)** is the transport equation for the turbulent dissipation rate, ε. The term P_k is the production term of turbulent energy due to the Reynolds stress. The term G_k is the production term of the turbulent energy by buoyancy. The buoyancy production term G_k is expressed in **Eq. (6)**, and the turbulent heat flux $-\overline{\theta u_j}$ in the equation is modeled by **Eq. (7)** in SGDH. As a remedy, it is conceivable to newly model $-\overline{\theta u_j}$ in **Eq. (9)**. In the GGDH analysis, the Reynolds stress $-\overline{u_i u_j}$ was set to **Eq. (10)** such that G_k is modeled using **Eq. (11)**, and the horizontal temperature–velocity gradient is also considered.

Tab. 3 – Turbulence model

$$\frac{\partial k}{\partial t}+\frac{\partial k U_i}{\partial x_i}=\frac{\partial}{\partial x_i}\left[\left(\nu+\frac{\nu_t}{\sigma_k}\right)\frac{\partial k}{\partial x_i}\right]+P_k+G_k-\varepsilon \quad \cdots(4)$$

$$\frac{\partial \varepsilon}{\partial t}+\frac{\partial \varepsilon U_i}{\partial x_i}=\frac{\partial}{\partial x_i}\left[\left(\nu+\frac{\nu_t}{\sigma_\varepsilon}\right)\frac{\partial \varepsilon}{\partial x_i}\right]+\frac{\varepsilon}{k}\left[C_{\varepsilon 1}(P_k+C_{\varepsilon 3}G_k)-C_{\varepsilon 2}\varepsilon\right] \cdots(5)$$

$$G_k=-\beta g_i\overline{\theta u_i} \quad \cdots(6) \qquad -\overline{\theta u_i}=\frac{\nu_t}{P_t}\frac{\partial \Theta}{\partial x_i} \quad \cdots(7)$$

$$G_k=-\beta g_z\frac{\nu_t}{P_t}\frac{\partial \Theta}{\partial z} \quad \cdots(8) \qquad -\overline{\theta u_i}=\frac{3\nu_t}{2P_t k}\overline{u_i u_j}\frac{\partial \Theta}{\partial x_j} \quad \cdots(9)$$

$$-\overline{u_i u_j}=\nu_t\left(\frac{\partial U_i}{\partial x_j}+\frac{\partial U_j}{\partial x_i}\right)-\frac{2}{3}\delta_{ij}k \quad \cdots(10)$$

$$G_k=-\beta g_z\frac{3\nu_t}{2P_t k}\left(\overline{wu}\frac{\partial \Theta}{\partial X}+\overline{wv}\frac{\partial \Theta}{\partial Y}+\overline{ww}\frac{\partial \Theta}{\partial z}\right) \quad \cdots(11)$$

ν: Kinematic viscosity$[m^2/s]$	ν_t: Eddy kinematic viscosity$[m^2/s]$
σ_k,σ_ε,C_{ε_1}, C_{ε_2}, C_{ε_3} : model constants	$\sigma_k = 1.0, \sigma_\varepsilon = 1.3,$ $C_{\varepsilon_1} = 1.44, C_{\varepsilon_2} = 1.92,$ $C_{\varepsilon_3} = 0.2$
C_μ: model parameter [=0.09]	
g_i: Gravitational acceleration vector [m^2/s^2]	
P_t: Turbulent Prandtl number [-]	
δ_{ij}: Kronecker delta dimensionless [-]	

2.4 Comparison of measurement and CFD analysis

Focusing on the installation height of the exhaust hood (1.0 m), we compared the analysis and actual experimental results. **Figure 5** shows the temperature difference distribution. From **Eq. (12)**, the temperature is arranged by an approximate equation based on the difference t between the plume and environmental temperatures and the radial distance r from the center of the thermal plume. The maximum temperature difference of the measured data was taken as the central axis temperature t_c, and the temperature distribution width R_t was determined using the least-squares method.

$$t/t_c = e^{-(r/R_t)^2} \quad \cdots(12)$$

When GGDH was used for all thermal powers, the CFD results were closer to the experimental results than SGDH. At a thermal power of 4.6 kW, the analysis results using the GGDH were almost in agreement with the experimental results. **Figure 6** shows the velocity distribution. The analysis values and the experimental results corresponded to each other for all thermal powers, but the results demonstrated that the analysis values using the GGDH diffused.

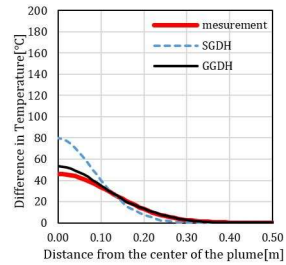

4.6 kW

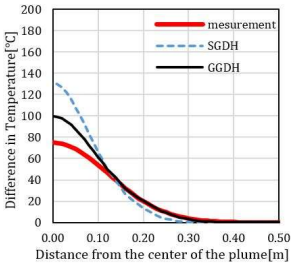

9.2 kW

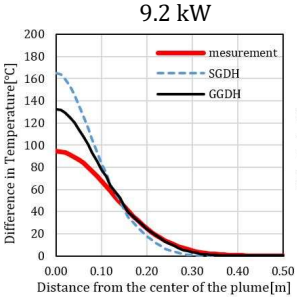

12.7 kW

Fig. 5 - Difference in temperature

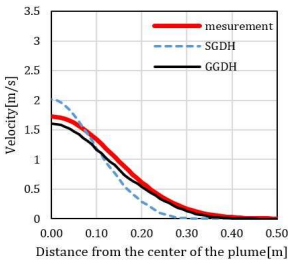

4.6kW

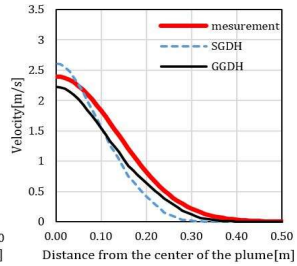

9.2 kW

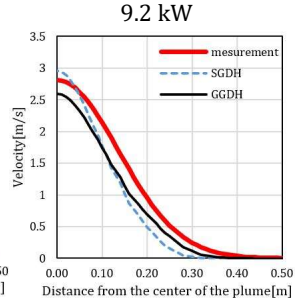

12.7 kW

Fig. 6 – Velocity

Figures 7 and **8** show the temperature difference and velocity on the central axis under the condition of a thermal power of 4.6 kW. **Figures 9** and **10** also show the results of plotting R_t and R_v at each height. The GGDH exhibited a value close to the measured result compared with the SGDH. The central axis velocity approached the experimental results as the height increased. From these findings, it can be concluded that the prediction accuracy was improved by CFD in an open flame.

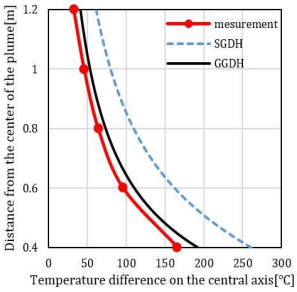

Fig. 7 - Temperature Difference on the central axis

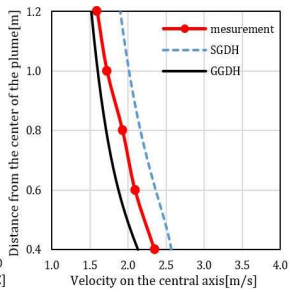

Fig. 8 – Velocity on the central axis

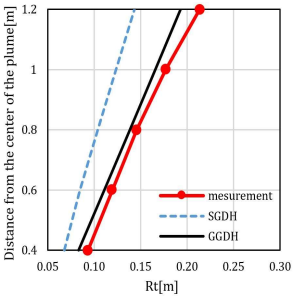

Fig. 9 - Temperature distribution width

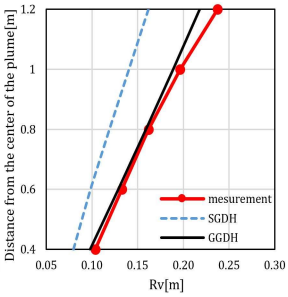

Fig. 10 – Velocity distribution width

3. Reproduction of Capture Efficiency

3.1 Measurement overview

The capture efficiency of the exhaust hood was measured according to the JSTM standards[6]. The capture efficiency of hood exhaust is measured separately for combustion exhaust gas generated from a gas-cooking appliance and for cooking products such as water and oil. For the combustion exhaust gas, carbon dioxide emitted from the gas-cooking appliance was used as a tracer gas. The capture efficiency of the hood exhaust was calculated using **Eq. (13)**.

$$\eta_C = \frac{C_{h,\infty}}{C_{h,100}} \quad \ldots(13)$$

The term η_C denotes the capture efficiency of the hood exhaust, $C_{h,\infty}$ is the average of the 10 min exhaust duct concentration, $C_{h,100}$ is the exhaust duct concentration measured with 100% capture of contamination from cooking equipment (complete collection state). **Figure 11** shows a section view of the test room used for the collection rate measurement. An exhaust hood of 0.90 m × 1.2 m × 0.68 m in height was installed on the gas stove.

The same commercial gas stove as in **Chapter *2.1*** was installed, and the target burners and thermal power were set under the same conditions.
The ventilation rates of the exhaust hood were determined as 391.5, 522, 652.5, and 783 m^3/h .

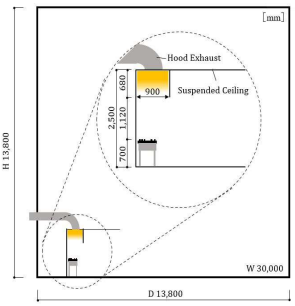

Fig. 11 – Test room

3.2 Overview of CFD analysis of capture efficiency

Figure 12 shows the analysis model. To reduce the analysis load, a part of the laboratory in the large space to be analyzed was targeted for analysis, and a wall surface other than the side wall adjacent to the gas stove was set as a slip boundary.

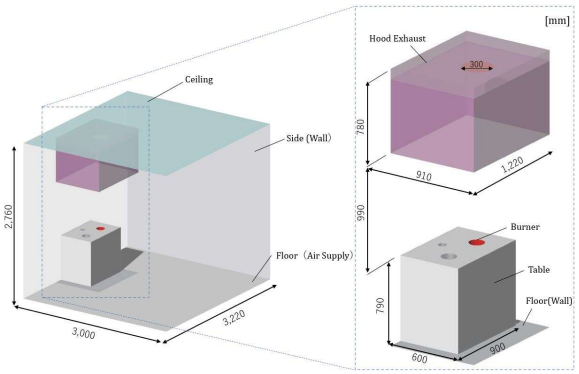

Fig. 12 – CFD analysis model of capture efficiency

Tab. 4 lists the boundary conditions. The floor surface was supplied with air, air was blown vertically upward at 0.10 m/s, and the ceiling surface was used as the pressure boundary. The boundary conditions for the burner were the same as in **Chapter *2.2* .**

Tab. 4 – Boundary conditions (capture efficiency)

Boundary	Type		
Burner	4.6 kW	Temperature	520 ℃
		Velocity	1.16 m/s
	9.2 kW	Temperature	814 ℃
		Velocity	2.00 m/s
	12.7 kW	Temperature	1006 ℃
		Velocity	2.62 m/s
	Material : Air Turbulent intensity : 0.25 Turbulent length scale : 0.10 m		
Floor	Velocity inlet (Temperature: 20℃, Velocity: 0.1 m/s, Turbulent intensity : 0.01 Turbulent length scale : 0.10 m)		
Ceiling	Boundary (Pressure: 0.00 Pa)		
Side Table	All dependent variable : 0 gradient condition		

3.3 Comparison of measurement and CFD analysis

Figures 13, 14, and **15** show a comparison of the results for capture efficiency. Under all thermal power conditions, CFD analysis using the SGDH as the turbulence model tended to overestimate the capture efficiency. In addition, the analysis results using the GGDH exhibited values close to the actual experimental results. In particular, under the conditions of thermal power of 9.2 and 12.7 kW, it was confirmed that the measurements were almost the same as those of GGDH regardless of the ventilation volume.

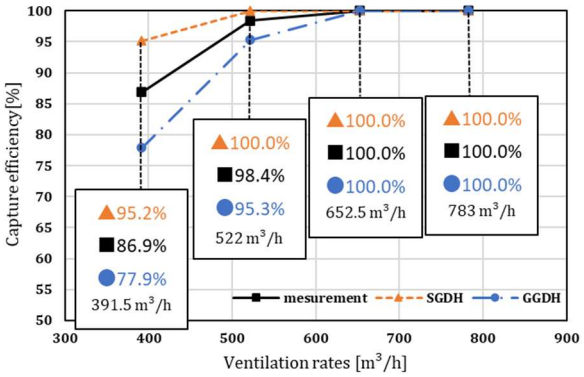

Fig. 13 - Comparison of capture efficiency of 4.6 kW

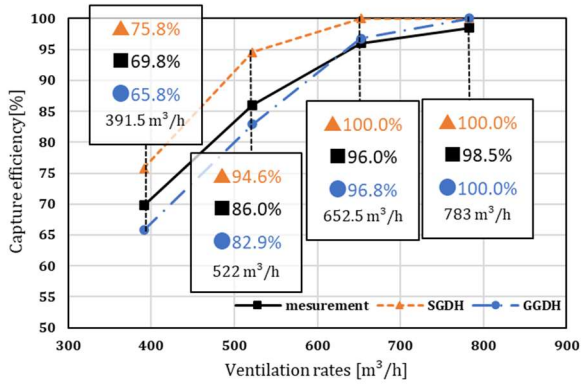

Fig. 14 - Comparison of capture efficiency of 9.2 kW

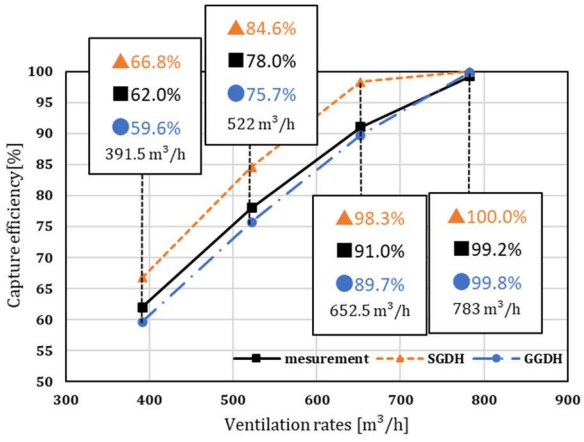

Fig. 15 - Comparison of capture efficiency of 12.7 kW

4. Conclusions

The following findings were obtained from this study:

(1) Using the generalized k–ε model (GGDH), it was confirmed that the temperature distribution of the thermal plume was closer to the measured value than that of the standard k–ε model (SGDH).

(2) Using the GGDH, it was confirmed that the collection rate of the exhaust hood was close to the measured value.

(3) When predicting the exhaust collection rate by CFD analysis in a commercial kitchen, it is important to use the GGDH as a turbulence model.

Reproducing the capture efficiency by CFD will be a material for future modeling and will significantly contribute to the comfort and energy saving of commercial kitchens in the long run.

In the future, boundary conditions should be set when the pot is installed on the stove. It is important to reflect the heat-transfer phenomena observed around the pot in CFD and improve the reproducibility of the plume. In addition, this research may be reflected in the actual Japanese kitchen environment in the future.

5. References

[1] Y. Kondo et al., Study on Air-Conditioning and Ventilation System od Kitchen (Part4) Numetrical Simulations of Flow and Temperature Distributions and Ventilation Efficiency, The Society of Heating, Air-Conditioning and Sanitary Engineers of Japan, proceedings, C-17, 1994, 201-204

[2] T. Momose et al., Measurement and Modeling of Plume above Commercial Cooking Stoves, The Architectural Institute of Japan's Journal of Environmental Engineering, No.567, 2003, 49-56

[3] J. Sakaguchi et al., Study on the Themal Environment and Air Flow Distribution in the House Kitchen by CFD analysis, Architectual Institute of Japan, Summaries of technical papers of annual meeting, 2008

[4] H.Kiyosuke et al., Study on reproduction of heat updraft on gas stove by CFD, Architectual Institute of Japan, Summaries of technical papers of annual meeting, 2018

[5] K. Van Maele et al., Application of two buoyancy-modified k–ε turbulence models to different types of buoyant plumes, Engineering Applications of Computational Fluid Mechanics, 2006

[6] JSTM V 6201: Measurement method for capture efficiency of exhaust hoods in commercial kitchens, 2017